indirect link-movement can be estimated from the regression line, $\chi = -90° + 0.48\phi'$.

Conclusion

The present study has proposed a method to formulate conformational movements using the circular correlation and regression analyses for the torsion angles of nucleosides and nucleotides. As a result, high correlations have been found in ϕ'-χ, χ-ϕ, χ-τ_0, τ_3-ψ', and ψ'-ϕ'. The link-movements of these pairs can be visualized in a scheme (Table III). This diagram implies that movements of a torsion angle can be transmitted one after another, and eventually one conformation is changed to another one. In other words, if any torsion except ψ is given a value, an entire conformational model can be built by transmitted operations using regression lines listed in Table III. During the operations, the conformation about the exocyclic C4'-C5' bond may be fixed to be gauche-gauche, because this conformation is strongly favored in crystals of nucleotides.

In general, the molecular structures of nucleosides or nucleotides have been regarded as conformationally "rigid"[21] probably due to the small variances of torsion angles. However, within their conformationally allowed regions, it was clearly shown that, in many cases, changes in two torsion angles have a functional relation. The simultaneous changes of any paired torsions in a nucleotide are likely to be regularly governed by the combinations of their regression lines. Certain pairs of torsion angles which were known to be correlated so far[1-4] have now been parameterized. We here understand conformational changes could be explained quantitatively by concerted movements of the paired torsion angles.

Acknowledgment. We thank Dr. M. Tanemura of the Institute of Statistical Mathematics, Tokyo, for his valuable discussions. We are also indebted to Dr. N. Yasuoka of Crystallographic Research Center, Institute for Protein Research, Osaka University, for the use of the computer. The crystallographic data used for the present work were retrieved with use of TOOL-IR system,[22] for which we thank Dr. T. Yamamoto of Tokyo University.

(21) Sundaralingam, M. In "Proceedings of the 5th Jerusalem Symposium Quantum Chemistry and Biochemistry", Bergmann, E. D., Pullman, B., Eds.; Academic Press: New York, 1973; pp 417-455.

(22) Yamamoto, T.; Negishi, N.; Ushimaru, M.; Tozawa, Y.; Okabe, K.; Fujiwara, S. "TOOL-IR An On-Line Information Retrieval System at an Inter-University Computer Center", Proceedings of the 2nd USA-Japan Computer Conference, 1975; pp 159-165.

Mechanism of the Reduction and Oxidation Reaction of Cytochrome *c* at a Modified Gold Electrode

W. John Albery,*[1a] Mark J. Eddowes,[1b] H. Allen O. Hill,*[1b] and A. Robert Hillman[1a]

Contribution from the Inorganic Chemistry Laboratory, South Parks Road, Oxford, England, and the Department of Chemistry, Imperial College, London, England. *Received November 18, 1980*

Abstract: The reduction and oxidation of cytochrome *c* at a gold electrode modified with an adsorbed layer of 4,4'-bipyridyl has been investigated by using rotating-disk and ring-disk electrodes. The current voltage curves for both the oxidation and reduction reactions show that the system is nearly reversible, but the rotation speed dependences of the limiting currents in either direction indicate that there are additional potential independent rate-limiting processes before and after the electron transfer. From the dependence of the limiting currents on the concentration of reactant and product, we deduce that there is considerable adsorption of both reactant and product. This adsorption step appears to be essential for rapid electron transfer between the electrode and the protein and the adsorption and desorption rates are rapid, as expected from the near reversibility of the overall electrode process. The adsorption of both reactant and product was also measured by using a ring-disk electrode with modulation of the disk current. From these results a free-energy profile for the overall electrode reaction is deduced. This free-energy profile is symmetrical and the three transition states are of about equal energy at the standard electrode potential of cytochrome *c*. The relationship between the binding of cytochrome *c* to the modified electrode and its interaction with its physiological redox partners is discussed.

Rapid electron transfer between electrodes and metalloproteins in general has proved difficult to achieve. However, as we have shown,[2] cytochrome *c* will undergo a rapid and reversible electrode reaction, corresponding to oxidation and reduction of the heme iron, at a gold electrode in the presence of 4,4'-bipyridyl, which appears to act by adsorbing on the electrode surface, thus providing a suitable interface for interaction with the protein. Direct-current and ac cyclic voltammetry indicates[3] that the electrode process is quasi-reversible and is essentially diffusion controlled. Alternating-current impedance measurements[4,5] have provided a value for the standard electrochemical rate constant, showing that the electrode reaction is indeed fast with $k_s = 1.5 \times 10^{-4}$ ms^{-1}. These studies have indicated[4,5] a specific binding interaction between cytochrome *c* and the modified electrode surface. Using rotating-disk and ring-disk techniques we have further investigated this proposed interaction and its effects on the kinetics of the observed electrode reaction.

Experimental Section

Rotating-disk voltammograms were recorded by point-by-point current measurement by using a 4-mm-diameter gold disk electrode in a 20-mL glass cell, incorporating a conventional three-electrode system, supplied by Oxford Electrodes Ltd. The gold working electrode was polished briefly before each experiment to remove surface contaminants by using a 1-μm alumina suspension in distilled water and then washed with distilled water. The reference electrode was a saturated calomel electrode (Radiometer, Type K 401) and the counter electrode was a platinum gauze, separated from the bulk solution by a fine glass frit. All potentials are reported with respect to the saturated calomel electrode. The potential and rotation speed of the electrode were controlled by a potentiostat and a rotating-disk rig, both supplied by Oxford Electrodes. The

(1) (a) Department of Chemistry, Imperial College; (b) Inorganic Chemistry Laboratory, University of Oxford.
(2) Eddowes, M. J.; Hill, H. A. O. *J. Chem. Soc., Chem. Commun.* **1977**, 771-772.
(3) Eddowes, M. J.; Hill, H. A. O. *J. Am. Chem. Soc.* **1979**, *101*, 4461-4464.
(4) Eddowes, M. J.; Hill, H. A. O.; Uosaki, K. *J. Am. Chem. Soc.* **1979**, *101*, 7113-7114.
(5) Eddowes, M. J.; Hill, H. A. O.; Uosaki, K. *Bioelectrochem. Bioenerg.* **1980**, *7*, 527-537.

0002-7863/81/1503-3904$01.25/0

Scheme I

$$A_\infty \underset{k_D}{\overset{k_D}{\rightleftharpoons}} A_0 \qquad \text{transport in solution}$$

$$A_0 \underset{\Gamma_L k_{des\cdot A}}{\overset{k_{ads\cdot A}}{\rightleftharpoons}} A_{ads} \qquad \text{adsorption and desorption of reactant}$$

$$A_{ads} \underset{\Gamma_L k_{-e}}{\overset{\Gamma_L k_e}{\rightleftharpoons}} B_{ads} + e \qquad \text{electron transfer}$$

$$B_{ads} \underset{k_{ads\cdot B}}{\overset{\Gamma_L k_{des\cdot B}}{\rightleftharpoons}} B_0 \qquad \text{desorption and adsorption of product}$$

$$B_0 \underset{k_D}{\overset{k_D}{\rightleftharpoons}} B_\infty \qquad \text{transport in solution}$$

rotation speed dependences of the limiting currents were similarly determined by point-by-point current measurement by using the above equipment. The ring–disk studies were carried out as previously described.[6] A gold–gold ring–disk electrode with the following radii was used: $r_1 = 1.985$ mm, $r_2 = 2.104$ mm, and $r_3 = 2.250$ mm. The rotation speed in these experiments was 10 Hz. The roughness factor of the electrode was determined by integrating the surface oxide peak in a cyclic voltammogram, assuming[7] that 1 cm^2 requires 400 μC.

Horse heart cytochrome *c* (Type VI) was obtained from the Sigma Chemical Co. and, in the oxidized form, was purified by the method of Brautigan et al.[8] The reduced form was prepared by reduction of purified ferricytochrome *c* with dithionite followed by desalting by gel filtration with Sephadex G25 (Pharmacia). Protein concentrations were determined from their visible absorption[9] at 520 and 550 nm. All other reagents used were of Analar grade. The supporting electrolyte used throughout was 0.1 M $NaClO_4$ with 0.02 M phosphate buffer, pH 7.

Proposed Reaction Scheme

As mentioned briefly above, our previous studies[4,5] have indicated a binding interaction between cytochrome *c* and the surface modified electrode, which parallels the proteins interaction[10,11] with its physiological redox partners in the mitochondrial respiratory chain. By analogy with its physiological redox reactions, in which a protein–protein complex is formed[12,13] prior to electron transfer, we propose a similar multistep mechanism for the electrode reaction of cytochrome *c* in which it binds to the electrode surface before the electron-transfer event itself can occur. As we will show, the rates of the various steps of this proposed reaction sequence, shown in Scheme I, account for the kinetics of the overall electrode process observed at the rotating-disk electrode. Scheme I represents the reaction $A \rightleftharpoons B + e$, where A is ferrocytochrome *c*, B is ferricytochrome *c*, and Γ_L/mol m^{-2} is the number of adsorption sites per unit area on the modified electrode. The various rate constants describe the rates of the following processes: k_D/ms^{-1} is the mass transport rate constant for a rotating-disk electrode, describing the transport of material from the bulk of solution to the electrode, and is given by the Levich eq[14]

$$k_D = 1.55D^{2/3}\nu^{-1/6}W^{1/2} = BW^{1/2} \qquad (1)$$

where W is the rotation speed in hertz. The rate constants $k_{ads\cdot A}$ and $k_{ads\cdot B}$ describe the rates of adsorption of the reduced and oxidized forms of cytochrome *c* and have the usual dimensions of the electrochemical rate constant. The rate constants k_e and k_{-e} are the potential dependent rate constants for the forward and backward electron-transfer reactions between adsorbed species and the electrode in units of s^{-1}, and are given by

$$k_e = k_e^\circ \exp[\alpha(nF/RT)(E - E^\circ)] \qquad (2a)$$

for the anodic process and

$$k_{-e} = k_e^\circ \exp[-\beta(nF/RT)(E - E^\circ)] \qquad (2b)$$

for the cathodic process, where k_e° is the standard first-order electron-transfer rate constant between adsorbed species and the electrode at the standard electrode potential of the system, E°. The coefficients α and β are the normal anodic and cathodic charge transfer coefficients. The constants $k_{des\cdot A}$ and $k_{des\cdot B}$ describe the rates of desorption of the reduced and oxidized forms of cytochrome *c* and are also in units of s^{-1}.

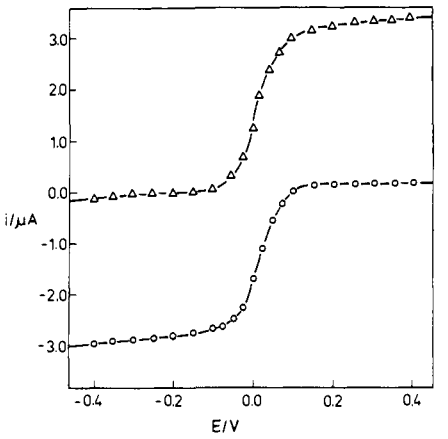

Figure 1. Typical current voltage curves for the oxidation (Δ) and reduction (O) of cytochrome *c* at a rotating gold disc electrode modified with 4,4′-bipyridyl. Rotation speed, $W = 25$ Hz.

Theory for Steady-State Experiments

We now derive equations for the proposed reaction scheme which describes the dependence of current on potential and rotation speed observed in the steady state at the rotating-disk electrode. Concentrations of species A and B are indicated by lower case letters. We can write the following equations for the flux, j(mol m^{-2} s^{-1}), of A to B:

$$\begin{aligned} j &= k_D(a_\infty - a_0) \\ &= k_{ads\cdot A}(1 - \theta_a - \theta_b)a_0 - \Gamma_L k_{des\cdot A}\theta_a \\ &= \Gamma_L k_e \theta_a - \Gamma_L k_{-e}\theta_b \\ &= \Gamma_L k_{des\cdot B}\theta_b - k_{ads\cdot B}(1 - \theta_a - \theta_b)b_0 \\ &= k_D(b_0 - b_\infty) \end{aligned} \qquad (3)$$

where θ_a and θ_b are the fraction of sites occupied by A and B, respectively. Elimination of θ_a, θ_b, a_0, and b_0 by equating these flux equations gives the general result:

$$\begin{aligned} j^{-1}(k_{ads\cdot A}k_e k_{des\cdot B}\Gamma_L a_\infty - k_{ads\cdot B}k_{-e}k_{des\cdot A}\Gamma_L b_\infty) = \\ k_D^{-1}\Gamma_L(k_{ads\cdot A}k_e k_{des\cdot B} + k_{des\cdot A}k_{-e}k_{ads\cdot B}) + \Gamma_L(k_e k_{des\cdot B} + \\ k_{-e}k_{des\cdot A} + k_{des\cdot B}k_{des\cdot A}) + \\ k_{ads\cdot A}a_\infty(k_e + k_{-e} + k_{des\cdot B}) + k_{ads\cdot B}b_\infty(k_e + k_{-e} + k_{des\cdot A}) + \\ jk_D^{-1}[(k_3 + k_{-e})(k_{ads\cdot B} - k_{ads\cdot A}) + k_{des\cdot A}k_{ads\cdot B} - k_{ads\cdot A}k_{des\cdot B}] \end{aligned} \qquad (4)$$

When the electrode is sufficiently positive k_e will be so large and k_{-e} correspondingly small that terms containing k_e will dominate and the limiting flux, j_l, will be observed and is described by

$$\frac{a_\infty}{j_l} = \frac{1}{k_D} + \frac{1}{k_{ads\cdot A}} + \frac{a_\infty}{\Gamma_L k_{des\cdot B}} + \frac{k_{ads\cdot B}b_\infty}{\Gamma_L k_{ads\cdot A}k_{des\cdot B}} + \frac{j_l(k_{des\cdot B} - k_{des\cdot A})}{\Gamma_L k_D k_{ads\cdot A}k_{des\cdot B}} \qquad (5)$$

In this expression the first three terms describe possible rate-limiting steps in the reaction: the transport to the electrode, the adsorption step, and the desorption step, respectively. The last two terms describe the competition of A and B for adsorption sites

(6) Albery, W. J.; Compton, R. G.; Hillman, A. R. *J. Chem. Soc., Faraday Trans. 1* **1978**, *74*, 1007–1019.
(7) Michri, A. A.; Pshchenichnikov, A. G.; Burshtein, R. Kh. *Elektrokhimiya* **1972**, *8*, 364–365.
(8) Brautigan, D. L.; Ferguson-Miller, S.; Margoliash, E. *Methods Enzymol.* **1978**, *53*, 128–164.
(9) Margoliash, E.; Frowit, N. *Biochem. J.* **1959**, *71*, 570.
(10) Ferguson-Miller, S.; Brautigan, D. L.; Margoliash, E. *J. Biol. Chem.* **1978**, *253*, 149–159.
(11) Rieder, R.; Bosshard, H. R. *FEBS Lett.* **1978**, *92*, 223–226.
(12) Nicholls, P.; Chance, B. In "Molecular Mechanisms of Oxygen Activation"; Hayaishi, O., Ed., Academic Press: New York, 1974; pp 479–534.
(13) Petersen, L. C.; Nicholls, P.; Degn, H. *Biochim. Biophys. Acta* **1976**, *452*, 59–65.
(14) Levich, V. G. "Physicochemical Hydrodynamics"; Prentice Hall: Engelwood Cliffs, NJ, 1962.

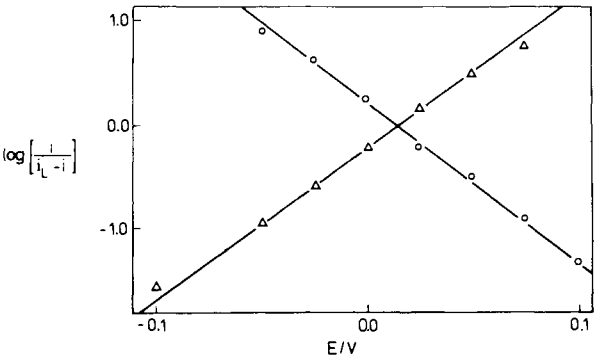

Figure 2. Plots according to eq 6 of the data in Figure 1.

Table I. Results from the Plots in Figure 2[a]

	$E_{1/2}$, mV	α_{obsd}
reduction of ferricytochrome *c*	15	0.92
oxidation of ferrocytochrome *c*	14	0.89

[a] W = 25 Hz; cytochrome *c* concentration, 160 μM.

on the electrode and in particular the term containing b_∞ describes product inhibition.

Results

Current Voltage Curves. Typical current voltage curves for the reduction of ferricytochrome *c* and the oxidation of ferrocytochrome *c* obtained by using a rotating gold disk electrode with 4,4′-bipyridyl in solution are shown in Figure 1. The corresponding plots according to eq 6 where i_L is the observed limiting

$$\log\left[\frac{i}{(i_L - i)}\right] = \text{a constant} \pm \frac{\alpha_{obsd} EF}{2.3RT} \qquad (6)$$

current are shown in Figure 2. Values of the half-wave potential, $E_{1/2}$, determined from the intercept on the potential axis and the coefficient α_{obsd} from the slope of these plots are reported in Table I. The values of $E_{1/2}$ are the same for both the anodic and cathodic processes and coincide with the previously reported[3,15,16] value for the formal electrode potential. The values of the experimental parameter, α_{obsd}, which for a fully reversible process should be equal to unity ($=\alpha + \beta$), and for an irreversible process should equal α for the anodic reaction and β for the cathodic reaction, are found to be close to unity. These facts suggest that the system is almost completely reversible. The values of α_{obsd} will be further discussed below.

Rotation Speed Dependence of Limiting Current. We find that the rotation speed dependence of limiting current, i_L, for both the oxidation and reduction reactions of cytochrome *c* does not obey the usual Levich equation[14] in which i_L varies linearly with $W^{1/2}$. This shows that the limiting current is not purely determined by transport and that, as we will now show, the adsorption and desorption rate terms in eq 5 influence the overall rate of the electrode process. Equation 5 does not correspond to the form of the Koutecky–Levich equation[17]

$$i^{-1} = \text{a constant} + B^{-1}W^{-1/2} \qquad (7)$$

frequently applicable where preceding chemical steps are encountered. We therefore rearrange eq 5 to obtain

$$(i_L^{-1} - i_{Lev}^{-1}) = \frac{1}{FAa_\infty}\left[\frac{1}{k_{ads\cdot A}} + \frac{a_\infty}{\Gamma_L k_{des\cdot B}} + \frac{k_{ads\cdot B} b_\infty}{\Gamma_L k_{ads\cdot A} k_{des\cdot B}} + \left(\frac{i_L}{i_{Lev}}\right)\left(\frac{(k_{ads\cdot B} - k_{ads\cdot A})a_\infty}{\Gamma_L k_{ads\cdot A} k_{des\cdot B}}\right)\right] \qquad (8)$$

where $i_{Lev} = FABW^{1/2} a_\infty$ and is the diffusion-controlled current predicted by the Levich equation. Plots of $(i_L^{-1} - i_{Lev}^{-1})$ against

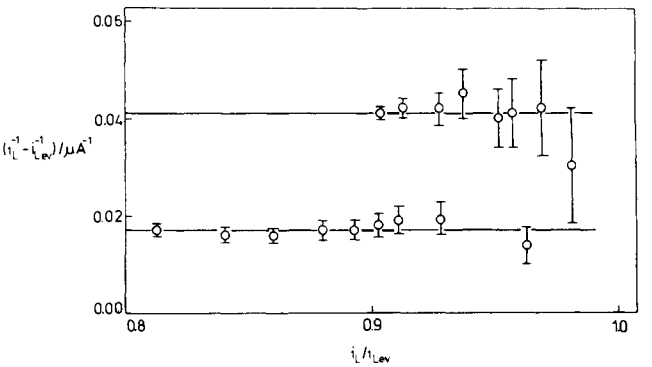

Figure 3. Typical plots, according to eq 8, of the observed limiting current, i_L, and the calculated current from the Levich equation, i_{Lev}, at rotation speeds between 4 and 49 Hz. Since the gradients are essentially zero, we conclude that $k_{ads\cdot A} = k_{ads\cdot B}$.

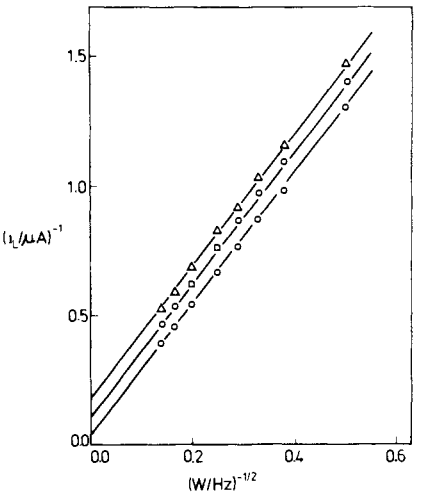

Figure 4. Typical Koutecky–Levich plots, according to eq 9, of the limiting current, i_L, against rotation speed, W; these were obtained for the oxidation of ferrocytochrome *c* (86 μmol dm^{-3}) in the presence of different concentrations of ferricytochrome *c* (b_∞): (○), 0 μmol dm^{-3}, (□) 105 μmol dm^{-3}, (△) 225 μmol dm^{-3}.

i_L/i_{Lev} are shown in Figure 3. Within experimental error the gradient of these plots is essentially zero, showing that, under these conditions, $k_{ads\cdot B}$ is approximately equal to $k_{ads\cdot A}$. With this assumption, eq 8 simplifies to a form of the Koutecky–Levich equation:

$$i_L^{-1} = (FAa_\infty)^{-1}\left[\frac{1}{BW^{1/2}} + \frac{1}{k_{ads}} + \frac{a_\infty}{\Gamma_L k_{des\cdot B}} + \frac{b_\infty}{\Gamma_L k_{des\cdot B}}\right] \qquad (9)$$

The terms in the square bracket represent the possible rate-limiting steps: transport of reactant to the electrode, adsorption of reactant onto the electrode, desorption of product, and product inhibition due to competition for adsorption sites, respectively. Plots of i_L^{-1} against $W^{1/2}$ are linear, and typical results are shown in Figure 4. From the gradients of these plots, for both reduction and oxidation, we use eq 9 to obtain a value for the diffusion coefficient of cytochrome *c*, $D = 1.1 \times 10^{-10}$ m^2 s^{-1}. This value is in good agreement with those obtained previously.[3,18,19] From eq 9 the intercept, I, of the Koutecky–Levich plot corresponds to the rate of the surface step in the electrode reaction and is given, for oxidation, by

$$I = (FA)^{-1}\left[\frac{1}{k_{ads}a_\infty} + \frac{1}{\Gamma_L k_{des\cdot B}} + \frac{b_\infty}{a_\infty \Gamma_L k_{des\cdot B}}\right] \qquad (10)$$

In the absence of product in bulk solution ($b_\infty = 0$), I should vary linearly with the reciprocal of concentration of the reactant (a_∞^{-1}).

(15) Henderson, R. W.; Rawlinson, W. A. *Biochem. J.* **1956**, *62*, 21–29.
(16) Hawkridge, F. M.; Kuwana, T. *Anal. Chem.* **1973**, *45*, 1021–1027.
(17) Koutecky, J.; Levich, V. G. *Zh. Fiz. Khim.* **1958**, *32*, 1565–1575.
(18) Theorell, H. *Biochem. Z.* **1936**, *285*, 207–218.
(19) Ehrenberg, A. *Acta Chem. Scand.* **1957**, *11*, 1257–1270.

Table II. Values of Adsorption and Desorption Rate Constants Obtained from the Koutecky-Lewis Plots

	oxidation	reduction
	Variation of Reactant	
gradient	$\frac{k_{ads\cdot A}}{ms^{-1}} = (2.3 \pm 0.3) \times 10^{-4}$	$\frac{k_{ads\cdot B}}{ms^{-1}} = (3.3 \pm 0.1) \times 10^{-4}$
intercept	$\frac{\Gamma_L k_{des\cdot B}}{mol\ m^{-2}\ s^{-1}} = (6.3 \pm 0.4) \times 10^{-5}$	$\frac{\Gamma_L k_{des\cdot A}}{mol\ m^{-2}\ s^{-1}} = (5.9 \pm 0.4) \times 10^{-5}$
	Variation of Product	
	$\frac{\Gamma_L k_{des\cdot B}}{mol\ m^{-2}\ s^{-1}} = (3.5 \pm 0.5) \times 10^{-5}$	

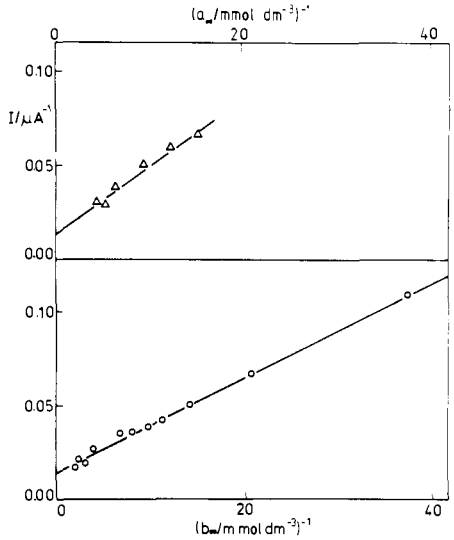

Figure 5. Variation of the intercept, I, of the Koutecky–Levich plots with reactant concentration according to eq 10 for oxidation (upper diagram) and reduction (lower diagram) of cytochrome c.

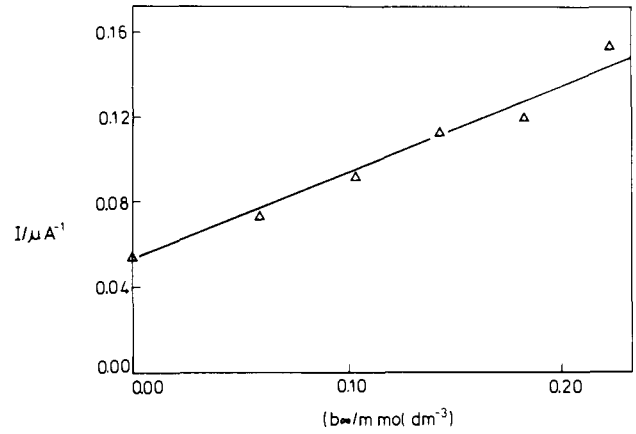

Figure 6. Variation of the intercept, I, of the Koutecky–Levich plots with product concentration at constant reactant concentration for the oxidation of ferrocytochrome c (86 μmol dm^{-3}) (as shown in Figure 4).

Figure 5 shows this variation for both the oxidation and reduction of cytochrome c. The values of $k_{ads\cdot A}$, $k_{ads\cdot B}$, $\Gamma_L k_{des\cdot A}$, and $\Gamma_L k_{des\cdot B}$ obtained from the slopes and intercepts of these plots by application of eq 10 are given in Table II. Furthermore, eq 10 predicts that the reaction should be inhibited by addition of the product to the bulk solution. Figures 4 and 6 illustrate the effect on the current due to oxidation of ferrocytochrome c of added ferricytochrome and show that, for a constant value of a_∞, I varies linearly with b_∞ as predicted by eq 10. A value of $\Gamma_L k_{des\cdot B}$ is also obtained from analysis of these data and is given in Table II. It can be seen that there is reasonable agreement between the values of $\Gamma_L k_{des\cdot B}$ and $\Gamma_L k_{des\cdot A}$ determined by varying either the reactant or the product concentrations.

Alternating-Current Ring–Disk Experiments. Experiments in which the disk current is modulated and the phase shift and amplitude of the corresponding ring current are measured provide a sensitive method for measuring adsorption of both reactant and product on the disk electrode.[20,21] A major advantage of the ring–disk technique is that the potential of the ring electrode can be selected so that the ring monitors either the reactant or the product. This means that the adsorption of reactant and product can be measured independently. Conventional ac impedance techniques do not allow this distinction to be made.[21]

In the ac ring–disk experiments, ferricytochrome c was reduced at the electrode with no ferrocytochrome c present in the bulk solution. The dc component of the disk current was set to half the value of the limiting current and the current was modulated about this value. The ring electrode was set to detect either the product of the disk reaction, ferrocytochrome c (a collection efficiency experiment), or the reactant of the disk reaction, ferricytochrome c (a shielding experiment). The amplitude of the modulated ring current is described by the complex collection efficiency[21] N_ω, where

$$N_\omega = N_F \cdot N_{tr} \tag{11}$$

In this expression N_{tr} describes the effect of the transport of species from the disk to the ring on the amplitude and phase shift of the ring current and is a known function[21,22] of the electrode geometry and the normalized frequency, ω', where

$$\omega' = 1.57(\nu/D)^{1/3}(fr/W) \tag{12}$$

and fr is the ac frequency in hertz.

Hence, from the observed N_ω and the calculated N_{tr} we can find the Faradaic component, N_F, which describes the amplitude and phase shift of the flux of either ferricytochrome c or ferrocytochrome c at the disk electrode with respect to the disk current. For a simple adsorption we have shown[21] that

$$N_F^{-1} - 1 = [K' k_D f(\omega')]/D \tag{13}$$

where

$$f(\omega') = \sqrt{\frac{\omega'}{2}} \times \left(\frac{\sinh \sqrt{2}\omega' - \sin \sqrt{2}\omega' - i(\sinh \sqrt{2}\omega' + \sin \sqrt{2}\omega')}{\cosh \sqrt{2}\omega' + \cos \sqrt{2}\omega'} \right) \tag{14}$$

and K'(m) describes the equilibrium at the disk electrode between the concentration in the solution of the species detected at the ring electrode and its concentration on the disk electrode surface. Figure 7 shows typical plots of the modulus of $(N_F^{-1} - 1)$ against the modulus of $f(\omega')$. Good straight lines are found, with comparable slopes and intercepts, regardless of whether the ring electrode is detecting ferricytochrome c or ferrocytochrome c.

(20) Albery, W. J.; Davis, A. H.; Mason, A. *Faraday Discuss. Chem. Soc.* **1973**, *56*, 317–329.

(21) Albery, W. J.; Hillman, A. R. *J. Chem. Soc., Faraday Trans. 1* **1979**, *75*, 1623–1634.

(22) Albery, W. J.; Drury, J. S.; Hutchinson, A. P. *Trans. Faraday Soc.* **1971**, *67*, 2414–2418.

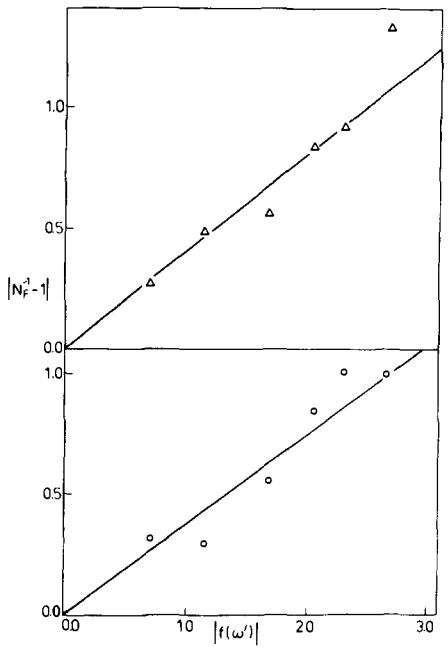

Figure 7. Variation of the amplitude of the Faradaic response found from the ring current, $N_F^{-1} - 1$, with the frequency function $f(\omega')$ (defined by eq 12 and 14) plotted according to eq 13. For the data in the upper diagram (△) the ring electrode was oxidizing ferrocytochrome *c* and in the lower diagram (○) it was reducing ferricytochrome *c*; in both cases the disk electrode was set at the half-wave potential for the reduction of ferricytochrome *c*.

Since the current is modulated about the half-wave potential, the mean surface concentrations of ferricytochrome *c* and ferrocytochrome *c* at the disk are equal, and hence this suggests that the free-energy profile for the adsorption/desorption reaction is essentially symmetrical, as indicated by the rotating-disk kinetics, and that

$$k_{ads\text{-}A}/\Gamma_L k_{des\text{-}A} = k_{ads\text{-}B}/\Gamma_L k_{des\text{-}B} = K \qquad (15)$$

In eq 15 K is the equilibrium constant for adsorption on the electrode in accordance with the Langmuir isotherm and, for a single substance, is given by

$$K = \theta/(1 - \theta)c \qquad (16)$$

Experiments were carried out in which we varied the concentration of ferricytochrome *c* from 16 to 215 μM in order to see how the adsorption varies with concentration. The general expression for $f(\omega')$ for the reaction Scheme I is cumbersome, but for the symmetrical system studied about its half-wave potential, the expression simplifies to the result in eq 13 and 14, and for Langmuir type adsorption we obtain[21]

$$1/\sqrt{K'} = 1/\sqrt{K}\sqrt{\Gamma_L} + \sqrt{K}\cdot b_0/\sqrt{\Gamma_L} \qquad (17)$$

Values for $K'^{-1/2}$ from eq 13 are plotted against b_0 ($=b_{\infty/2}$) in Figure 8.

Since the system is symmetrical, we can determine values of K' from ac impedance measurements at low frequency. These have been analyzed according to the equation previously presented[21] with

$$Q = 2p^2K'k_D/D(1 + p) \qquad (18)$$

and $p = 1$.

Reasonable agreement is found between values for K' determined from the different experiments. From the slope and intercept of the plots derived from the ring–disk experiments (Figure 8) we obtain

$$\Gamma_L = 1.2 \times 10^{-6} \text{ mol m}^{-2}$$

$$K = 2 \times 10^4 \text{ mol}^{-1} \text{ dm}^3$$

We can estimate a value of Γ_L from the cross-sectional area of

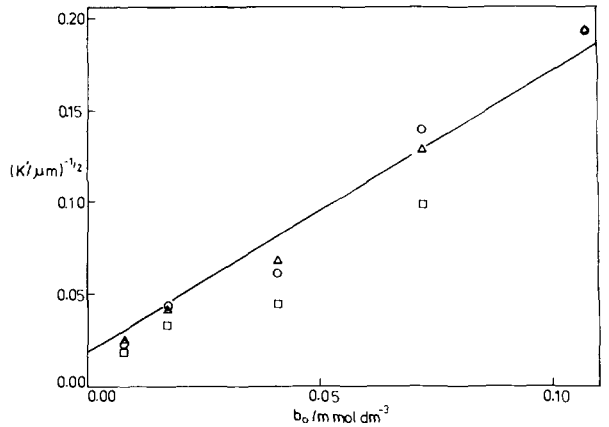

Figure 8. Langmuir isotherms plotted according to eq 17 for the adsorption of ferricytochrome *c* (○) and ferrocytochrome *c* (△) where K' has been measured from the gradients of plots such as those in Figure 7. Points from the conventional impedance analysis, according to eq 18, are shown as □.

cytochrome *c*. Assuming it to be a sphere of radius 1.5 nm and taking into account the measured roughness factor of the electrode of 4, we obtain

$$\Gamma_L = 0.9 \times 10^{-6} \text{ mol m}^{-2}$$

and this value is in good agreement with those measured experimentally.

We can also compare the results with those obtained from the Koutecky–Levich plots given in Table II. From the ring–disk experiments we obtain

$$K = 2 \times 10^4 \text{ mol}^{-1} \text{ dm}^3$$

whereas from Table II we find

$$K = 0.3 \text{ to } 1 \times 10^4 \text{ mol}^{-1} \text{ dm}^3$$

Thus fair agreement is found between the values determined by the two quite different experiments.

Analysis of the Current vs. Potential Relationship. We may now consider the values of the coefficient α_{obsd} in Table I, determined from the plots in Figure 2. For the system in which $k_{ads\text{-}A} = k_{ads\text{-}B}$ and $k_{des\text{-}A} = k_{des\text{-}B}$ and with $b_\infty = 0$, the general eq 4 reduces to

$$\frac{i_L}{i} = 1 + \frac{k_{-e}}{k_e} + \frac{k_{des}}{k_e}\left(1 - \frac{i_L}{i_{Lev}}\right) \qquad (19)$$

Writing k_e and k_{-e} in terms of k_e° and the relevant exponential functions of potential gives, after rearrangement, an expression for the potential dependence of the current function $\log [i/(i_L - i)]$. Differentiation shows that the slope of the plot according to eq 6 at $E_{1/2}$ is given by

$$\alpha_{obsd} = 1 - \beta/\left[1 + \frac{k_e^\circ}{k_{des}}\left(\frac{i_{Lev}}{i_{Lev} - i_L}\right)\right] \qquad (20a)$$

for the anodic reaction and

$$\alpha_{obsd} = 1 - \alpha/\left[1 + \frac{k_e^\circ}{k_{des}}\left(\frac{i_{Lev}}{i_{Lev} - i_L}\right)\right] \qquad (20b)$$

for the cathodic reaction. Hence, using the result in Table I, we see that since the values of α_{obsd} are the same for the anodic and cathodic processes $\alpha = \beta = 1/2$, and so, applying eq 20 to the data in Table I, we find that

$$k_e^\circ/k_{des} = 0.5$$

Using the value of k_{des} and Γ_L determined from the adsorption studies, we find

$$k_e^\circ = (30 \pm 5) \text{ s}^{-1}$$

This result may be compared with the value of k_e° calculated from the previously reported value[4,5] for the standard electrochemical

Table III. Values of Rate Constants

$k_{ads\cdot A} = k_{ads\cdot B} = 3 \times 10^{-4}$ ms^{-1}
$k_{des\cdot A} = k_{des\cdot B} = 50$ s^{-1}
$k_e^\circ = k_{-e}^\circ = 50$ s^{-1}
$\Gamma_L = 1.2 \times 10^{-6}$ mol m^{-2}
$K = 5 \times 10^3$ mol^{-1} dm^3

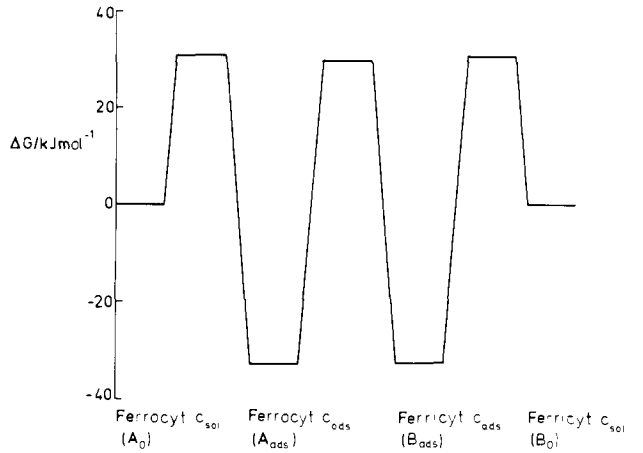

Figure 9. The free-energy profile for the reduction and oxidation of cytochrome *c* at a gold electrode, modified with 4,4′-bipyridyl, held at a potential, $E = E^\circ$.

rate constant, k_s. The two electrochemical rate constants are related by

$$k_s = \frac{K\Gamma_L k_e^\circ}{[1 + K(a_\infty + b_\infty)]} = (1.4\text{–}1.9) \times 10^{-4} \text{ ms}^{-1} \quad (21)$$

Substituting in values for K, Γ_L, a_∞, and b_∞, we find

$$k_e^\circ = 75\text{–}100 \text{ s}^{-1}$$

Considering the very different methods of obtaining these values, the agreement between the two values of k_e° is good.

In Table III we collect together our final estimates of the rate constants for the system.

Free-Energy Profile. At $E = E^\circ$ the free energies of activation for the various steps in the reaction may be calculated by application of the usual transition-state theory expression, $k = Z \exp(-\Delta G^\ddagger/RT)$. For the adsorption step, the frequency factor, Z, is 10^2 ms^{-1}, which is that used in the Marcus treatment,[23] and for the first-order electron-transfer and desorption-rate constants, the frequency factor is the usual kT/h. We obtain the following values for the free energies of activation: adsorption, $\Delta G^\ddagger = 31$ kJ mol^{-1}, desorption and electron transfer, $\Delta G^\ddagger = 63$ kJ mol^{-1}. The free-energy profile is shown in Figure 9.

Discussion

Perhaps the most striking feature of the free-energy profile (Figure 9) is that the binding energy is considerable and is, in fact, the reason why the electron-transfer reaction of cytochrome *c* proceeds at a measurable rate at the modified gold electrode. The overall rate of electron transfer is determined by the distribution of the protein at the surface and the probability of electron transfer between the electrode and species at the surface. In a situation where the binding energy of the protein to the surface is zero, the equilibrium constant for binding is given by the ratio of the frequency factors for k_{ads} and k_{des} and corresponds to a distribution of species determined by statistical probability. Thus we may calculate for this case the standard electrochemical rate constant, $k_s = 10^{-9}$ ms^{-1}, which is indeed slow and may account for the fact that the electron-transfer reaction between the unmodified electrode and cytochrome *c* is not observed when using normal voltammetric techniques. On the other hand, at the modified electrode surface, because of the large binding energy, the overall probability of electron transfer is greatly increased, accounting for the observed rate,[4,5] $k_s = 1.5 \times 10^{-4}$ ms^{-1}.

In general, rapid electron transfer between metalloproteins in solution and electrodes is not observed. It may also be noted that, where measurable rates of electron transfer have been observed[24,25] between the mercury electrode and cytochrome *c* or[26,27] other metalloproteins, adsorption of the protein onto the electrode surface is also observed. We therefore suggest that the reaction scheme outlined in Scheme I be a general one for the electron-transfer reactions of metalloproteins at electrodes and that, in order to overcome the substantial activation energy for electron transfer itself, a considerable binding energy for the preceding adsorption step is essential. Such a mechanism may also explain the anomalously low diffusion coefficient determined from the polarographic studies of cytochrome *c*, in which the limiting current was assumed to be purely diffusion controlled. In the presence of the preceding adsorption step, the limiting current is controlled, not only by diffusion but also by the adsorption step. The limiting current will be lower than that predicted for pure diffusion control and this will lead to a measured diffusion coefficient lower than the true value.

The binding of cytochrome *c* to the modified electrode surface provides a striking analogy with its binding to its physiological redox partners. We have suggested[4,5] that this analogous behavior is a result of the lysine residues around the exposed heme edge being responsible for the binding interaction in both the case of the electrode reaction and the physiological reactions of cytochrome *c*. This binding interaction is presumably due to hydrogen bonding of the protein lysine residues to the adsorbed 4,4′-bipyridyl nitrogen lone pairs in the former case and to the carboxyl residues of its redox partner in the latter.[10,11] Thus in either reaction the heme edge will be oriented toward its electron donor or acceptor so as to facilitate the electron-transfer process. The free-energy profile in Figure 9 supports these suggestions and underlines the importance of the binding step.

The electrode reaction of cytochrome *c*, by its analogy with the physiological redox reactions of the protein, carries important implications for the latter. The efficient functioning of the mitochondrial respiratory chain, or any other biological electron-transport chain, requires that electron transfer occur rapidly between a protein and its immediate partners, though not to other redox proteins in the chain. The redox centers between which these electron transfers occur frequently lie a comparatively large distance apart[28,29] and the mechanism by which rapid rates of electron transfer between them is achieved has been the subject of much discussion.[30] The importance of the binding energy may similarly apply in the physiological redox reactions, where again rapid overall rates of electron transfer are observed. In biological systems the binding step may fulfill two important roles. First, it can overcome a large free-energy barrier for electron transfer between proteins in which the redox centers lie a considerable distance apart. Secondly, it can confer specificity on the redox reactions, allowing electron transfer between only those proteins which bind sufficiently strongly. This would prevent electron transfer between two proteins which are not natural partners even though they may encounter each other during their normal function, thus ensuring that the electron follows its correct pathway.

The other striking features of the free-energy profile are firstly that it is essentially symmetrical and secondly that the three

(23) Marcus, R. A. *J. Phys. Chem.* **1963**, *67*, 853.
(24) Betso, S. R.; Klapper, M. H.; Anderson, L. B. *J. Am. Chem. Soc.* **1972**, *94*, 8197–8204.
(25) Scheller, F.; Janchen, M.; Lampe, J.; Prumke, H.-J.; Blanck, J.; Palacek, E. *Biochim. Biophys. Acta* **1975**, *412*, 157–167.
(26) Niki, K.; Yagi, T.; Inokuchi, H.; Kimura, K. *J. Am. Chem. Soc.* **1979**, *101*, 3335–3340.
(27) Kakutani, T.; Toriyama, K.; Ikeda, T.; Senda, M. *Bull. Chem. Soc. Jpn.* **1980**, *53*, 947–950.
(28) Leonard, J. J.; Yonetani, T. *Biochemistry* **1976**, *13*, 1465–1468.
(29) Gupta, R. K.; Yonetani, T. *Biochim. Biophys. Acta* **1973**, *292*, 502–508.
(30) See, for example, "Tunneling in Biological Systems", Chance, B.; De Vault, D. C.; Frauenfelder, H.; Marcus, R. A.; Schrieffer, J. R.; Sutin, N., Eds.; Academic Press: New York, 1979.

transition states are of roughly equal free energy. Perfect symmetry would mean that the binding energy of cytochrome *c* to the electrode is independent of its oxidation state. We have suggested[31] that the simplest mechanism to facilitate an enzyme-catalyzed reaction is for the enzyme to bind the substrate and product in a nondiscriminatory fashion and that equality in the free energies of the different transition states may be a feature of efficient enzymes reacting with their natural substates. Finally, it is interesting that, by use of the rotating-disk and ring–disk techniques, it is possible to obtain a free-energy profile for an electrochemical reaction including the kinetics of the adsorption and desorption steps.

(31) Albery, W. J.; Knowles, J. R. *Biochemistry* **1976**, *15*, 5631-5640.

Conclusions

The free-energy profile for the electron-transfer reaction of cytochrome *c* at the 4,4′-bipyridyl surface-modified gold electrode emphasizes the importance of the preceding binding step in the electron-transfer kinetics of cytochrome *c*. Furthermore, it suggests that, with the development of other, suitably modified electrode surfaces, it should prove possible to enhance the rates of electron transfer between electrodes and metalloproteins in general. Such surface-modified electrodes would be of use not only in the study of the electron-transfer mechanisms of metalloproteins but also in the exploitation of enzymes as electrocatalysts.

Acknowledgment. This is a contribution from the Oxford Imperial Energy Group. We thank the S.R.C., N.R.D.C., and Johnson Matthey Ltd. for financial assistance.

Model Studies for a Molecular Mechanism of Action of Oral Anticoagulants

Richard B. Silverman

Contribution from the Department of Chemistry, Northwestern University, Evanston, Illinois 60201. *Received August 18, 1980*

Abstract: Warfarin [3-(α-acetonylbenzyl)-4-hydroxycoumarin], a potent oral anticoagulant agent, is known to inhibit the enzyme vitamin K epoxide reductase (Whitlon et al., ref 18 b). The molecular mechanism of inhibition, however, is not known. It is proposed that the two major classes of oral anticoagulants, the 3-substituted-4-hydroxycoumarins and the 2-substituted-1,3-indandiones, are mechanism-based inactivators of this enzyme. The proposed mechanism of inactivation involves enzyme-catalyzed activation of the oral anticoagulants by tautomerization to the hypothetically reactive diketo forms which then undergo attack by active-site nucleophiles. In order to test the chemistry of this proposal, it is shown that the two classes of oral anticoagulants are unreactive toward bases and nucleophiles (except for deprotonation), until they are electrophilically substituted at the 3 position of the coumarins or at the 2 position of the indandiones. These model compounds for the proposed enzyme-generated reactive intermediates, then, are shown to be highly reactive toward a variety of nucleophiles and support the hypothesis that the oral anticoagulants are converted by vitamin K epoxide reductase into reactive compounds which can acylate an active-site nucleophile and thereby inactivate the enzyme.

The oral anticoagulants, i.e., 3-substituted-4-hydroxycoumarins (e.g., warfarin, **1b**) and 2-substituted-1,3-indandiones (e.g., phenindione, **2a**), are some of the most important drugs for the prevention and treatment of a variety of venous and, to a lesser extent, arterial thromboembolic disorders.[1] Fifty percent of hospitalized patients that die show evidence of antemortem thromboembolism. The first oral anticoagulant, Dicumarol (**1a**),

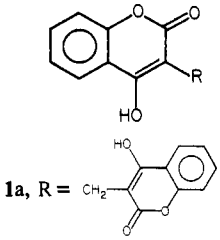

1a, R =

1b, R = $CH(Ph)CH_2COCH_3$
1c, R = CH_3

was isolated from spoiled sweet clover and was shown to be responsible for the hemorrhagic sweet clover disease of cattle.[2] That same year its structure was identified,[3] it was chemically synthesized[4] and was shown to be a clinically useful anticoagulant drug.[5] Numerous analogues of Dicumarol and of 4-hydroxycoumarins were synthesized and tested for anticoagulant activity.[6] Warfarin, 3-(α-acetonylbenzyl)-4-hydroxycoumarin (**1b**), origi-

Scheme I. Vitamin K–Vitamin K Epoxide Cycle (R = Phytyl)

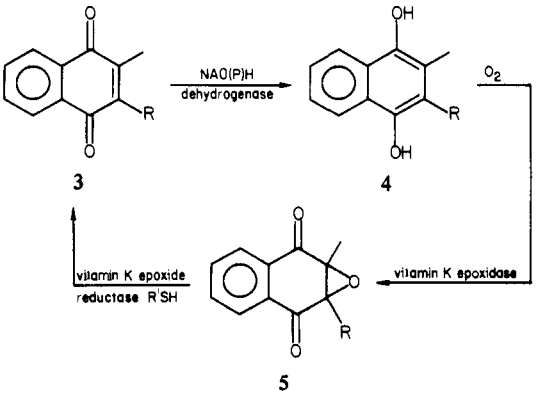

3 **4** **5**

(1) Levine, W. G. In "The Pharmacological Basis of Therapeutics", 5th ed., Goodman, L. S.; Gilman, A., Ed.; New York: MacMillan, 1975.
(2) Campbell, H. A.; Link, K. P. *J. Biol. Chem.* **1941**, *138*, 21.
(3) Stahmann, M. A.; Heubner, C. F.; Link, K. P. *J. Biol. Chem.* **1941**, *138*, 513.
(4) Huebner, C. F.; Link, K. P. *J. Biol. Chem.* **1941**, *138*, 529.
(5) Butt, H. R.; Allen, E. V.; Bollman, J. L. *Mayo Clinic Proc.* **1941**, *16*, 388.
(6) (a) Overman, R. S.; Stahmann, M. A.; Huebner, C. F.; Sullivan, W. R.; Spero, L.; Doherty, D. G.; Ikawa, M.; Graf, L.; Roseman, S.; Link, K. P. *J. Biol. Chem.* **1944**, *153*, 5; (b) O'Reilly, R. A. *Annu. Rev. Med.* **1976**, *27*, 245.

0002-7863/81/1503-3910$01.25/0